

## Macroscopic Quantum Test with Bulk Acoustic Wave Resonators

Björn Schriniski,<sup>1</sup> Yu Yang,<sup>2</sup> Uwe von Lüpke,<sup>2</sup> Marius Bild,<sup>2</sup> Yiwen Chu,<sup>2</sup> Klaus Hornberger,<sup>3</sup> Stefan Nimmrichter,<sup>4</sup> and Matteo Fadel<sup>2,\*</sup>

<sup>1</sup>Center for Hybrid Quantum Networks (Hy-Q), Niels Bohr Institute, University of Copenhagen, Blegdamsvej 17, DK-2100 Copenhagen, Denmark

<sup>2</sup>Department of Physics, ETH Zürich, 8093 Zürich, Switzerland

<sup>3</sup>University of Duisburg-Essen, Faculty of Physics, Lotharstraße 1, 47048 Duisburg, Germany

<sup>4</sup>Naturwissenschaftlich-Technische Fakultät, Universität Siegen, Walter-Flex-Straße 3, 57068 Siegen, Germany

 (Received 21 September 2022; accepted 15 February 2023; published 29 March 2023)

Recently, solid-state mechanical resonators have become a platform for demonstrating nonclassical behavior of systems involving a truly macroscopic number of particles. Here, we perform the most macroscopic quantum test in a mechanical resonator to date, which probes the validity of quantum mechanics by ruling out a classical description at the microgram mass scale. This is done by a direct measurement of the Wigner function of a high-overtone bulk acoustic wave resonator mode, monitoring the gradual decay of negativities over tens of microseconds. While the obtained macroscopicity of  $\mu = 11.3$  is on par with state-of-the-art atom interferometers, future improvements of mode geometry and coherence times could test the quantum superposition principle at unprecedented scales and also place more stringent bounds on spontaneous collapse models.

DOI: [10.1103/PhysRevLett.130.133604](https://doi.org/10.1103/PhysRevLett.130.133604)

Understanding the quantum-classical transition is one of the main challenges of modern physics. Is the Schrödinger equation valid all the way from the microscopic to the macroscopic world, with quantum effects increasingly hard to observe due to environmental decoherence [1]? Or do the laws of quantum mechanics break down at some point, so as to reinstate “macrorealism” in our everyday life [2]? This question is not philosophical, as it can be tackled by demonstrating genuine quantum effects in ever more macroscopic systems.

Single atoms have been delocalized over macroscopic length and timescales, reaching meters and seconds in state-of-the-art experiments [3–6]. On the other hand, molecule interferometry has pushed the mass boundaries by confirming the wave nature for compounds of more than  $10^4$  atomic mass units [7,8]. Future Earth- and space-based experiments with freely falling or levitated nanoparticles aim at even higher mass and timescales [9,10], but in such schemes it is a single rigid-body degree of freedom that is placed into a superposition.

This is to be contrasted with growing efforts in electro- and optomechanics toward demonstrating quantum states in the elastic deformation of condensed matter systems of substantially higher mass. Recent experimental milestones include the successful preparation of nonclassical states of surface and bulk acoustic modes, demonstrated through the observation of Wigner function negativities [11–15]. Such nonclassical states of motion involve a truly macroscopic number of atoms, on the order of  $10^{16}$ , vibrating in unison. At the same time, each atom is delocalized only over a tiny

fraction of the size of an atomic nucleus, which makes unclear how they compare to previous tests of the quantum-classical transition.

Using an objective measure for the degree of macroscopicity of nonclassical states [16], we report here the most macroscopic quantum test performed with a solid-state mechanical resonator. The macroscopicity value obtained in our experiment is surprisingly large, motivating us to optimize the design specifications for future electro-mechanical experiments to become competitive even with matter-wave superposition tests.

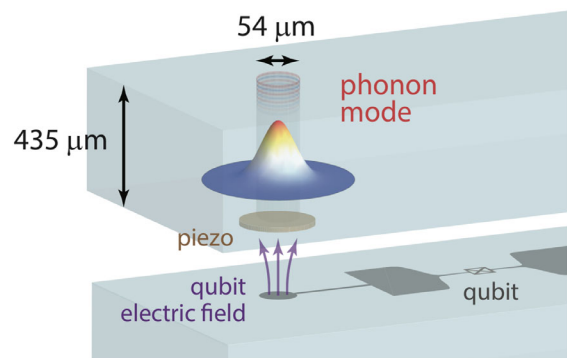


FIG. 1. Illustration of the HBAR device used in this work (not to scale, see Ref. [14] for details). A superconducting qubit couples to a mechanical acoustic mode localized in the bulk of a sapphire crystal through a piezoelectric material. This allows the preparation and measurement of the quantum state of the phonon mode.

To justify the macroscopicity measure used, note that any genuine quantum test probes the validity of quantum mechanics against the hypothesis of macrorealism, which is that a modification of quantum theory destroys coherence above a certain size or mass scale, rendering superposition phenomena unobservable in practice. Hence, the degree to which a quantum experiment falsifies a broad, generic class of minimally invasive, macrorealistic modifications of quantum mechanics gives rise to an objective benchmark [16]. Using the measurement data to rule out a range of values of the coherence time parameter  $\tau_e$  quantifying the macrorealist modification, an experiment is justifiably the more macroscopic the greater the  $\tau_e$  values falsified through Bayesian inference [17]. The macroscopicity measure  $\mu$  is then determined by the logarithm of the greatest ruled out  $\tau_e$  value [18]. To date, the highest macroscopicity  $\mu = 14$  has been achieved in molecule interferometry [8].

In our experiment, we observe Wigner function negativities for up to 40  $\mu\text{s}$  in an bulk acoustic vibration mode of a sapphire crystal with an effective mass of 1  $\mu\text{g}$ , which is prepared in a single-phonon state and in a superposition of Fock states. This quantum signature is detected by measuring the displaced parity [19] of the quantum state using a superconducting qubit; see Fig. 1. Our analysis shows that it can be associated with a large macroscopicity  $\mu = 11.3$ , despite the subnuclear delocalization of the atoms involved. Based on this, we explain how future experiments with bulk acoustic resonators may realize the most macroscopic quantum test.

*Macroscopicity of bulk resonator modes.*—To evaluate the macroscopicity of a demonstrated quantum effect, one should consider the class of macrorealistic models possibly falsified by the experiment. Keeping those models minimally invasive in that they preserve linearity, the semigroup nature of the time evolution, invariance under the chosen nonrelativistic reference frame, and other basic consistency principles [16], their observable impact can be formulated as a Lindblad generator  $\mathcal{L}\rho$  modifying the quantum evolution of the system state  $\rho$ . For a large compound of  $N \gg 1$  atomic constituents with masses  $m_1, \dots, m_N$ , the generator reduces to [16]

$$\mathcal{L}\rho = \frac{1}{\tau_e} \int d^3q g(q, \sigma_q) \mathcal{D}[\mathbf{L}(\mathbf{q})]\rho, \quad (1)$$

with  $\mathcal{D}[\mathbf{L}]\rho = \mathbf{L}\rho\mathbf{L}^\dagger - \{\mathbf{L}^\dagger\mathbf{L}, \rho\}/2$ . The strength of the modification is specified by the coherence time parameter  $\tau_e$  and the standard deviation  $\sigma_q$  of the isotropic Gaussian momentum distribution  $g(q, \sigma_q) = e^{-q^2/2\sigma_q^2}/(2\pi\sigma_q^2)^{3/2}$ . The Lindblad operators are mass-weighted sums of single-particle momentum kicks by  $\mathbf{q}$ ,  $\mathbf{L}(\mathbf{q}) = \sum_{n=1}^N (m_n/m_e) \times e^{i\mathbf{q}\cdot\mathbf{r}_n/\hbar}$ , with  $\mathbf{r}_n$  the particle position operators and  $m_e$  a reference mass chosen to be that of an electron.

We note that the theory of continuous spontaneous collapse (CSL) can be described by Eq. (1), but it is

usually parametrized in terms of a rate per atomic mass unit  $\lambda_{\text{CSL}} = (1 u/m_e)^2/\tau_e$ , and a localization length  $r_{\text{CSL}} = \hbar/\sqrt{2}\sigma_q$  [20]. The strongest bounds on these CSL parameters are currently achieved by so-called noninterferometric tests [21], where one measures the noise experienced by a classical system by exploiting the fact that macrorealistic modifications are accompanied by a heating effect. However, a genuine quantum signal, such as interference fringes or a negative Wigner function, is required for a CSL test to also probe the validity of quantum mechanics in the system.

In the following, we consider a collective acoustic excitation in the bulk condensed matter, taking the form

$$\mathbf{u}(\mathbf{r}) = \exp\left(-\frac{y^2 + z^2}{w_0^2}\right) \cos\left(\pi \frac{\ell x}{L}\right) \mathbf{e}_x \quad (2)$$

of waist  $w_0$ , mode index  $\ell$ , and length  $L$ . (The mode vanishes for  $x \notin [0, L]$ , and is laterally well confined within the material.) The effective volume of the mode is defined as  $V_{\text{eff}} = \int d^3r u^2(\mathbf{r}) = \pi w_0^2 L/4$  and, given the mass density  $\rho$ , the effective mass is defined as  $m_{\text{eff}} = \int d^3r \rho(\mathbf{r}) u^2(\mathbf{r})$ . This way one consistently obtains the total bulk volume and mass in the limiting case of a center of mass motion, corresponding to a uniform displacement with  $u(\mathbf{r}) = 1$ , so that  $m_{\text{eff}}$  can be understood as the mass fraction taking part in the displacement [22].

The mode is quantized by means of the ladder operator  $\mathbf{a} = (\mathbf{X} + i\mathbf{P})/\sqrt{2}$ , involving a conjugate pair of dimensionless position and momentum quadrature operators,  $[\mathbf{X}, \mathbf{P}] = i$ . A single phononic excitation thus displaces the atoms by amplitudes of the order of the zero-point fluctuation  $x_0/\sqrt{2}$ , with  $x_0 = \sqrt{\hbar/m_{\text{eff}}\omega}$ , around their equilibrium positions  $\mathbf{r}_n$  according to the mode displacement field, i.e.,  $\mathbf{r}_n = \mathbf{r}_n + \mathbf{u}(\mathbf{r}_n)x_0\mathbf{X}$ . The Lindblad operators thus become

$$\mathbf{L}(\mathbf{q}) = \frac{1}{m_e} \int d^3r \rho(\mathbf{r}) e^{i\mathbf{q}\cdot\mathbf{r}/\hbar} e^{i\mathbf{q}\cdot\mathbf{u}(\mathbf{r})x_0\mathbf{X}/\hbar}. \quad (3)$$

In the relevant regime of modification length scales  $\hbar/\sigma_q$  larger than the interatomic distances, it is safe to assume a homogeneous mass density  $\rho(\mathbf{r}) = \bar{\rho}$  and to expand the operator in Eq. (3) to first order in  $\mathbf{X}$  [17]. This results in momentum diffusion,  $\mathcal{L}\rho = 2\Gamma\mathcal{D}[\mathbf{X}]\rho$ , with a diffusion rate amplified by the effective oscillator mass,

$$\begin{aligned} \Gamma &= \frac{\bar{\rho}^2 x_0^2}{2m_e^2 \tau_e \hbar^2} \int d^3q g(q, \sigma_q) q_x^2 \left| \int d^3r u_x(\mathbf{r}) e^{i\mathbf{q}\cdot\mathbf{r}/\hbar} \right|^2 \\ &= \frac{m_{\text{eff}}^2 (4x_0/L)^2}{m_e^2 \tau_e (1 + \sigma_w^2)} \int d\zeta \frac{e^{-\zeta^2/2\sigma_L^2} (1 - (-)^\ell \cos \zeta)}{\sqrt{2\pi}\sigma_L (1 - \pi^2 \ell^2/\zeta^2)^2}. \end{aligned} \quad (4)$$

The rate depends on how the modification length scale  $\hbar/\sigma_q$  compares to the geometric length scales of the

oscillator mode, as determined by  $\sigma_w = w_0\sigma_q/\hbar$ ,  $\sigma_L = L\sigma_q/\hbar$ ,  $x_0$ , and  $\ell$ . The integral can be given analytically, leading to a lengthy expression for  $\Gamma$ . In the limit  $\sigma_L, \sigma_w \ll 1$  and for  $\ell$  even, we find  $\Gamma \propto m_{\text{eff}}\sigma_q^2\sigma_L^4/\ell^4$ , whereas for  $\sigma_L \gg \pi\ell$  and  $\sigma_w \gg 1$ , we get  $\Gamma \propto m_{\text{eff}}/\sigma_w^2$ . The maximum  $\Gamma$  with respect to  $\sigma_q$  is located in between at  $\hbar/\sigma_q \approx \sqrt{3}L/\pi\ell$ , provided that  $\pi\ell \gg 1$  and  $\pi\ell w_0/\sqrt{3}L \gg 1$  [22],

$$\max_{\sigma_q} \Gamma \approx \sqrt{\frac{3\pi}{2e^3}} \frac{6\hbar\bar{q}}{m_e^2\omega\tau_e} \frac{L}{\ell}. \quad (5)$$

Given a fixed sound velocity  $v$ , and noting  $\omega = 2\pi v\ell/L$ , the maximum rate value is proportional to the square of the mode wavelength  $L/\ell$ .

In the corotating frame of the oscillator, and including energy decay at rate  $\gamma_\downarrow$ , the modified time evolution of the oscillator state  $\rho$  is given by the master equation

$$\begin{aligned} \dot{\rho} &= \Gamma \mathcal{D}[\mathbf{a}e^{-i\omega t} + \mathbf{a}^\dagger e^{i\omega t}]\rho + \gamma_\downarrow \mathcal{D}[\mathbf{a}]\rho \\ &\approx (\Gamma + \gamma_\downarrow) \mathcal{D}[\mathbf{a}]\rho + \Gamma \mathcal{D}[\mathbf{a}^\dagger]\rho. \end{aligned} \quad (6)$$

In the second line we average over the rapidly oscillating cross terms, as we are interested in decoherence on time-scales much longer than the oscillation period.

The coarse-grained isotropic master equation, Eq. (6), admits a compact solution in the Wigner function representation

$$\begin{aligned} W(X, P; t) &= \frac{e^{\gamma_\downarrow t}}{\pi S(t)} \int dX' dP' W(X' e^{\gamma_\downarrow t/2}, P' e^{\gamma_\downarrow t/2}; 0) \\ &\times e^{-[(X-X')^2 + (P-P')^2]/S(t)}, \end{aligned} \quad (7)$$

with  $S(t) = (1 + 2\Gamma/\gamma_\downarrow)(1 - e^{-\gamma_\downarrow t})$ . This expression can be computed analytically for several states of interest, such as Fock states and their superposition [22]. Bayesian parameter estimation based upon Eq. (7) allows us to identify from the measured Wigner functions the threshold value  $\Gamma_{5\%}$  that corresponds to the most conservative 5% quantile of the coherence time  $\tau_e$  at any  $\sigma_q$  [17,22]. Greater  $\tau_e$  are also compatible with the data, as the observed decoherence might as well be due to unspecified conventional noise sources, but smaller times can be ruled out with confidence. Macroscopicity is then defined as follows. We convert  $\Gamma_{5\%}$  into the corresponding macrorealistic coherence time parameter  $\tau_e = \tau_e(\sigma_q, \Gamma_{5\%})$  by virtue of Eq. (4), maximize over  $\sigma_q$  to obtain the greatest excluded  $\tau_e$ , and assign a macroscopicity value  $\mu = \log_{10}(\tau_e/1 \text{ s})$ .

By modeling the state evolution with Eq. (6), we thus assume a zero-temperature environment and attribute any heating or decoherence beyond energy relaxation at the rate  $\gamma_\downarrow$  to the impact of a macrorealistic modification described by infinite-temperature diffusion at the rate  $\Gamma$ . This amounts

to a conservative assessment of the macroscopicity, since, by overestimating the hypothetical contribution of macrorealistic diffusion to the observed decoherence, we overestimate  $\Gamma$  and thus underestimate  $\tau_e$ . We characterize the energy relaxation rate  $\gamma_\downarrow$  independently, by a standard measurement of the phonon decay time  $T_1$  and the steady-state population [22].

*Experiment.*—Our measurements are carried out on a high-overtone bulk-acoustic wave resonator (HBAR) device cooled down at millikelvin temperature (see Fig. 1), which makes use of a superconducting qubit to prepare, control, and read out the quantum excitation of a mechanical mode localized in the bulk of a sapphire substrate [14].

The acoustic vibration mode is described to a very good approximation by Eq. (2), as also verified by numerical simulations. It oscillates over the bulk length  $L = 435 \mu\text{m}$  at angular frequency  $\omega = 2\pi \cdot 5.961 \text{ GHz}$  with wavelength  $\lambda = 1.8 \mu\text{m}$ , corresponding to the mode index  $\ell = 2L/\lambda = 486$ . Assuming a homogenous mass density  $\bar{\rho} = 3.98 \text{ g/cm}^3$ , and given the transverse waist  $w_0 = 27 \mu\text{m}$ , we obtain the effective oscillator mass  $m_{\text{eff}} = \pi w_0^2 L \bar{\rho} / 4 = 1.0 \mu\text{g}$  and a zero-point fluctuation of  $x_0/\sqrt{2} = 1.2 \times 10^{-18} \text{ m}$ . For these parameters, we find from Eq. (4) a maximal diffusion rate of  $\Gamma_{\text{max}} = 3.5 \times 10^{13}/\tau_e$  at a critical length scale  $\hbar/\sigma_q \approx 0.5 \mu\text{m}$ , which is of the same order as the mode wavelength.

The coherence properties of the phonon mode are characterized by a small one-phonon steady-state population of  $1.6 \pm 0.2\%$ , by the relaxation time  $T_1 = 85.8 \pm 1.5 \mu\text{s}$ , and by the Ramsey dephasing time  $T_2 = 147.3 \pm 2.6 \mu\text{s}$  [22]. These imply a much longer pure dephasing time of  $T_\phi = (1/T_2 - 1/2T_1)^{-1} = 1.0 \pm 0.2 \text{ ms}$ . Relaxation, which originates from the coupling to the environment through, e.g., surface scattering or diffraction loss, thus dominates the degradation of quantum features over time, and we can safely assume  $\gamma_\downarrow \approx 1/T_1$  within error tolerance.

Using the toolbox of circuit quantum acoustodynamics, we can use the qubit to prepare and measure the HBAR in nonclassical states of motion [11]. In particular, an arbitrary superposition with the first excited state,  $a|0\rangle + b|1\rangle$ , can be prepared by swapping the qubit state  $a|\downarrow\rangle + b|\uparrow\rangle$  to the mechanical mode through the resonant Jaynes-Cummings interaction. For any  $b \neq 0$  we obtain a nonclassical state of motion with negativities in the Wigner function that will degrade over time due to relaxation. To monitor this effect, we let the system evolve for a time  $t$ , and then obtain the Wigner function of the mechanical state by measuring its displaced parity [14,22]. Figure 2 shows how the measured Wigner function degrades over time for an initial Fock state  $|1\rangle$  (top row) and an initial superposition state  $(|0\rangle + |1\rangle)/\sqrt{2}$  (bottom row). Note the disappearance of negative (blue) regions in the quasiprobability distribution, turning it into a classical phase-space distribution.

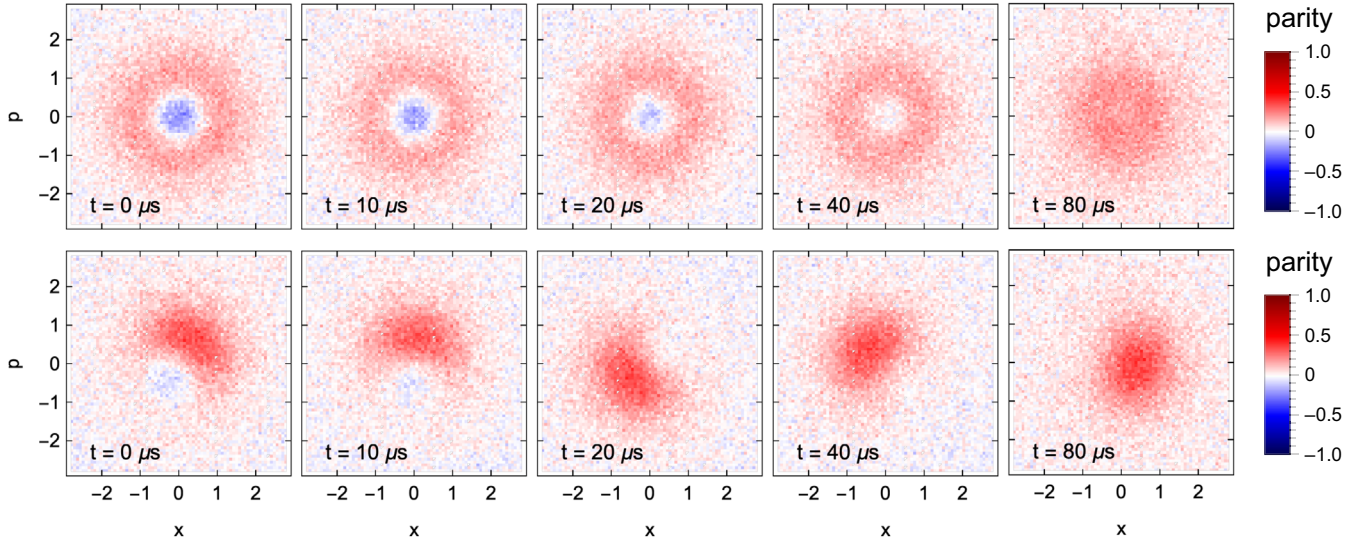


FIG. 2. Measured Wigner functions of a bulk acoustic mode initially prepared in the Fock state  $|1\rangle$  (top row) and in the superposition state  $(|0\rangle + |1\rangle)/\sqrt{2}$  (bottom row). Both states are initially nonclassical, as indicated by the phase space regions with negative quasiprobability (blue). As time evolves (left to right), both states approach the ground state  $|0\rangle$  due to relaxation. Comparing the measured data to the theoretical model Eq. (7) allows us to extract the maximal compatible diffusion rate  $\Gamma$  through Bayesian inference, yielding the macroscopicity  $\mu$  for the considered experiment.

In the first part of the experiment, we prepare the resonator in the single-phonon Fock state  $|1\rangle$  and measure its Wigner quasiprobability distribution as a function of time (Fig. 2, top row). We observe that the region of negative values around the phase-space origin shrinks gradually, persisting for tens of microseconds, before the Wigner function turns purely positive and becomes indistinguishable from a classical distribution. The longer and more pronounced the initial negativity remains, the stronger the experiment falsifies macrorealist modifications of quantum mechanics. We estimate the impact of such modifications by first fitting the initial measurement at  $t = 0$  with the Wigner function of an incoherent mixture of  $|0\rangle$  and  $|1\rangle$ , thus accounting for imperfections in the state preparation and measurement. The measured Wigner functions at  $t = 10 \mu\text{s}$ ,  $20 \mu\text{s}$ , and  $40 \mu\text{s}$  are then compared to the theoretical expectation, Eq. (7), including energy relaxation with the measured rate  $\gamma_{\downarrow} \approx 1/T_1$  as well as modification-induced diffusion with variable rate  $\Gamma$ . Bayesian parameter estimation and subsequent maximization with respect to  $\sigma_q$  shows that any  $\Gamma > \Gamma_{5\%} = 1.6 \times 10^2 \text{ s}^{-1}$  can be excluded with 95% confidence (at  $\hbar/\sigma_q \simeq 0.5 \mu\text{m}$ ) [22]. This corresponds to a macroscopicity of  $\mu = 11.3$ , by far the highest value reported on mechanical resonators; see Table I. We note that the obtained diffusion rate  $\Gamma_{5\%} = 1.6 \times 10^2 \text{ s}^{-1}$  is consistent with what is found by using our system to perform a so-called noninterferometric test of macrorealistic models based on the observed residual excitation of the mode [22]. Thus, our analytic results can be straightforwardly adopted in such schemes, as recently proposed in Ref. [30].

In the second part of the experiment, we prepare the resonator in the superposition state  $(|0\rangle + |1\rangle)/\sqrt{2}$ . As shown in the bottom row of Fig. 2, the measured Wigner function again takes negative values, confirming the nonclassicality of the initial state. The asymmetry around the origin, whose phase can be controlled by the qubit state, rotates due to a small detuning between the oscillator and the displacement pulse frequencies. This rotation is accounted for in our data processing. Following the previous analysis, we find that the superposition state data is compatible with a maximal diffusion rate of  $\Gamma_{5\%} = 6.4 \times 10^2 \text{ Hz}$ , which is a factor of 4 larger than the rate found from the Fock state  $|1\rangle$  and from the noninterferometric test [22]. This discrepancy can be explained by the presence of an additional pure dephasing channel with a rate of  $1/T_{\phi} \sim 10^3 \text{ Hz}$ . While circularly symmetric Wigner functions such as single Fock states are

TABLE I. Macroscopicities of solid-state mechanical resonator experiments reporting Wigner function negativities (\*, estimated), and most macroscopic matter-wave interference experiments assessed in [17,31]. The values with asterisks are estimates of what could have been observed based on the stated  $T_1$  time [22].

Experiment		Year	$\mu$
Mechanical resonators	<i>Bulk acoustic waves [this Letter]</i>	2022	11.3
	Phononic crystal resonator [13]	2022	$\sim 9.0^*$
	Surface acoustic waves [12]	2018	$\sim 8.6^*$
Matter-wave interference	Molecule interferometry [8]	2019	14.0
	Atom interferometry [6]	2019	11.8
	BEC interferometry [5]	2017	12.4

unaffected by this decoherence channel, which corresponds to a random rotation around the phase-space origin, a superposition of Fock states, which is necessarily asymmetric, gets washed out at rate  $1/T_\phi$ , removing any negativity. However, to fairly assess the macroscopicity of the Fock state superposition, we do *not* include this decoherence channel into the master equation, Eq. (6), so that all decoherence is attributed to the macrorealistic modification. This results in a greater diffusion rate, and consequently in a lower macroscopicity of  $\mu = 10.7$ . If we included the  $1/T_\phi$  dephasing effect in the Bayesian inference the resulting rate would be consistent with both the Fock state  $|1\rangle$  analysis and the noninterferometric test.

*Beating the macroscopicity record.*—Based on our experimental results, and using the analytical result, Eq. (4), we can now establish how to optimize future quantum experiments with bulk acoustic resonators to become competitive with the most macroscopic quantum tests to date. In contrast to quantum tests based on the interference of center-of-mass degrees of freedom, the diffusion rate scales here only weakly with the mass and length scales of the material: in the realistic case of comparable lateral and longitudinal mode extension ( $w_0 \approx L$ ), we find that macrorealistic diffusion is strongest at a length scale  $\hbar/\sigma_q$  comparable to the mode wavelength  $L/\ell$ . To attain greater macroscopicity in a given material, one should strive to increase the mode wavelength since the maximum diffusion rate, Eq. (5), grows like  $(L/\ell)^2$ . Apart from these geometric considerations, the macroscopicity also benefits from longer relaxation and coherence times  $T_1$ ,  $T_2$ , and a better characterization of the measurement noise. The latter can be incorporated into the Bayesian parameter estimation to extract better bounds, instead of adding a broad Gaussian noise channel as done in the analysis above.

As an example, keeping the same device and mode geometry as in the present experiment, but using a mode with  $\omega = 2\pi \times 2$  GHz and  $T_1 = 10$  ms, would result in  $\mu = 14.4$ , surpassing all reported quantum tests; see Table I. We obtain this estimate by setting  $\ell = 160$  and rescaling the observed coherence time in proportion to  $T_1$ ; the macroscopicity grows logarithmically with increasing coherence time. Beyond that, out-of-plane drum modes with frequencies in the low MHz range and huge quality factors have been reported, corresponding to  $T_1 > 100$  ms [32]. If genuine quantum effects could be demonstrated in these devices, they might reach substantially greater macroscopicities  $\mu > 17$  [33].

*Conclusion.*—We demonstrated the most macroscopic quantum test with bulk acoustic wave resonators, based on monitoring the time evolution of nonclassical Wigner functions. The reported macroscopicity is comparable to the one obtained by an experiment holding cesium atoms in a spatial superposition at 4  $\mu\text{m}$  separation over 20 s [6]. In the future, we envisage improved resonator designs that may surpass the most macroscopic matter wave

interferometers, testing the validity of quantum mechanics at unprecedented scales.

We would like to thank Georg Enzian and Eric Planz for helpful discussions. B. S. was supported by Deutsche Forschungsgemeinschaft (DFG, German Research Foundation), Grant No. 449674892. U. vL. is funded by the SNF Project No. 200021\_204073. M. F. was supported by The Branco Weiss Fellowship—Society in Science, administered by the ETH Zürich.

\*Corresponding author.

fadelm@phys.ethz.ch

- [1] M. Schlosshauer, Quantum decoherence, *Phys. Rep.* **831**, 1 (2019).
- [2] A. J. Leggett, Testing the limits of quantum mechanics: Motivation, state of play, prospects, *J. Phys. Condens. Matter* **14**, R415 (2002).
- [3] T. Kovachy, P. Asenbaum, C. Overstreet, C. A. Donnelly, S. M. Dickerson, A. Sugarbaker, J. M. Hogan, and M. A. Kasevich, Quantum superposition at the half-metre scale, *Nature (London)* **528**, 530 (2015).
- [4] S. Abend, M. Gebbe, M. Gersemann, H. Ahlers, H. Müntinga, E. Giese, N. Gaaloul, C. Schubert, C. Lämmerzahl, W. Ertmer, W. P. Schleich, and E. M. Rasel, Atom-Chip Fountain Gravimeter, *Phys. Rev. Lett.* **117**, 203003 (2016).
- [5] P. Asenbaum, C. Overstreet, T. Kovachy, D. D. Brown, J. M. Hogan, and M. A. Kasevich, Phase Shift in an Atom Interferometer Due to Spacetime Curvature Across its Wave Function, *Phys. Rev. Lett.* **118**, 183602 (2017).
- [6] V. Xu, M. Jaffe, C. D. Panda, S. L. Kristensen, L. W. Clark, and H. Müller, Probing gravity by holding atoms for 20 seconds, *Science* **366**, 745 (2019).
- [7] S. Eibenberger, S. Gerlich, M. Arndt, M. Mayor, and J. Tüxen, Matter-wave interference of particles selected from a molecular library with masses exceeding 10000 amu, *Phys. Chem. Chem. Phys.* **15**, 14696 (2013).
- [8] Y. Y. Fein, P. Geyer, P. Zwick, F. Kiałka, S. Pedalino, M. Mayor, S. Gerlich, and M. Arndt, Quantum superposition of molecules beyond 25 kda, *Nat. Phys.* **15**, 1242 (2019).
- [9] B. A. Stickler, B. Papendell, S. Kuhn, B. Schriniski, J. Millen, M. Arndt, and K. Hornberger, Probing macroscopic quantum superpositions with nanorotors, *New J. Phys.* **20**, 122001 (2018).
- [10] R. Kaltenbaek *et al.*, Research campaign: Macroscopic quantum resonators (MAQRO), *Quantum Sci. Technol.* **8**, 014006 (2023).
- [11] Y. Chu, P. Kharel, T. Yoon, L. Frunzio, P. T. Rakich, and R. J. Schoelkopf, Creation and control of multi-phonon Fock states in a bulk acoustic-wave resonator, *Nature (London)* **563**, 666 (2018).
- [12] K. J. Satzinger, Y. P. Zhong, H. S. Chang, G. A. Peairs, A. Bienfait, M.-H. Chou, A. Y. Cleland, C. R. Conner, É. Dumur, J. Grebel, I. Gutierrez, B. H. November, R. G. Povey, S. J. Whiteley, D. D. Awschalom, D. I. Schuster,

- and A. N. Cleland, Quantum control of surface acoustic-wave phonons, *Nature (London)* **563**, 661 (2018).
- [13] E. A. Wollack, A. Y. Cleland, R. G. Gruenke, Z. Wang, P. Arrangoiz-Arriola, and A. H. Safavi-Naeini, Quantum state preparation and tomography of entangled mechanical resonators, *Nature (London)* **604**, 463 (2022).
- [14] U. von Lüpke, Y. Yang, M. Bild, L. Michaud, M. Fadel, and Y. Chu, Parity measurement in the strong dispersive regime of circuit quantum acoustodynamics, *Nat. Phys.* **18**, 794 (2022).
- [15] M. Bild, M. Fadel, Y. Yang, U. von Lüpke, P. Martin, A. Bruno, and Y. Chu, Schrödinger cat states of a 16-microgram mechanical oscillator, [arXiv:2211.00449](https://arxiv.org/abs/2211.00449).
- [16] S. Nimmrichter and K. Hornberger, Macroscopicity of Mechanical Quantum Superposition States, *Phys. Rev. Lett.* **110**, 160403 (2013).
- [17] B. Schriniski, S. Nimmrichter, B. A. Stickler, and K. Hornberger, Macroscopicity of quantum mechanical superposition tests via hypothesis falsification, *Phys. Rev. A* **100**, 032111 (2019).
- [18] Note that the macrorealist modification hypothesis can be probed also in experiments that do not involve quantum superpositions. Only observations of genuine quantum signatures can therefore be assigned a benchmark value  $\mu$  [17]. This requires the interrogated state not to have an underlying classical description, excluding all oscillator states with positive Wigner function.
- [19] A. Royer, Wigner function as the expectation value of a parity operator, *Phys. Rev. A* **15**, 449 (1977).
- [20] A. Bassi, K. Lochan, S. Satin, T. P. Singh, and H. Ulbricht, Models of wave-function collapse, underlying theories, and experimental tests, *Rev. Mod. Phys.* **85**, 471 (2013).
- [21] M. Carlesso, S. Donadi, L. Ferialdi, M. Paternostro, H. Ulbricht, and A. Bassi, Present status and future challenges of non-interferometric tests of collapse models, *Nat. Phys.* **18**, 243 (2022).
- [22] See Supplemental Material at <http://link.aps.org/supplemental/10.1103/PhysRevLett.130.133604> for details on the experimental setup and the theoretical calculations, including Refs. [23–29].
- [23] H. Jeffreys, An invariant form for the prior probability in estimation problems, *Proc. R. Soc. A* **186**, 453 (1946).
- [24] P. Arrangoiz-Arriola, Quantum acoustics with lithium niobate nanostructures, Ph.D. thesis, Stanford University, 2019.
- [25] K. J. Satzinger, Quantum control of surface acoustic wave phonons, Ph.D. thesis, UC Santa Barbara, 2018.
- [26] K. J. Satzinger, (private communication).
- [27] Y. Chu, P. Kharel, W. H. Renninger, L. D. Burkhardt, L. Frunzio, P. T. Rakich, and R. J. Schoelkopf, Quantum acoustics with superconducting qubits, *Science* **358**, 199 (2017).
- [28] M. Armano, H. Audley, G. Auger, J. Baird, M. Bassan, P. Binetruy, M. Born, D. Bortoluzzi, N. Brandt, M. Caleno *et al.*, Sub-Femto-*g* Free Fall for Space-Based Gravitational Wave Observatories: Lisa Pathfinder Results, *Phys. Rev. Lett.* **116**, 231101 (2016).
- [29] M. Carlesso, A. Bassi, P. Falferi, and A. Vinante, Experimental bounds on collapse models from gravitational wave detectors, *Phys. Rev. D* **94**, 124036 (2016).
- [30] G. Tobar, S. Forstner, A. Federov, and W. P. Bowen, Testing spontaneous wavefunction collapse with quantum electromechanics, [arXiv:2206.14531](https://arxiv.org/abs/2206.14531).
- [31] B. Schriniski, S. Nimmrichter, and K. Hornberger, Quantum-classical hypothesis tests in macroscopic matter-wave interferometry, *Phys. Rev. Res.* **2**, 033034 (2020).
- [32] Y. Seis, T. Capelle, E. Langman, S. Saarinen, E. Planz, and A. Schliesser, Ground state cooling of an ultracoherent electromechanical system, *Nat. Commun.* **13**, 1507 (2022).
- [33] This rough estimate is based on [17], by approximating the mode in [32] as the fundamental Bessel mode  $\mathbf{u}(\mathbf{r}) = J_0(4.81\sqrt{y^2 + z^2}/d)\mathbf{e}_x$ , for a disk with diameter  $d = 100\ \mu\text{m}$ , 14 nm thickness, and  $m_{\text{eff}} \simeq 68\ \text{pg}$ . Precise  $\mu$  values would depend on a combination of effective mass, mode profile, and observed duration of Wigner negativities.